ISSN 2075-1087, Gyroscopy and Navigation, 2017, Vol. 8, No. 1, pp. 1–14. © Pleiades Publishing, Ltd., 2017.
Published in Russian in Giroskopiya i Navigatsiya, 2016, No. 4, pp. 76–97.

Comprehensive Overview of Quickest Detection Theory and its Application to GNSS Threat Detection

D. Egea-Roca*, G. Seco-Granados, and J.A. López-Salcedo

Universitat Autònoma de Barcelona (UAB), Barcelona, Spain

**e-mail: Daniel.Egea@uab.cat*

Received May 5, 2016

Abstract—Local threats such as radio frequency interference, multipath and spoofing have attracted the attention of many researchers in the past years thus leading to a myriad of contributions in the field of threat detection. Nevertheless, the current state of the art relies on classical detection techniques, which are not well suited for threat detection. In this paper, we take a leap forward by adopting the so-called quickest detection framework. This approach fits perfectly in critical applications where the aim is to detect the presence of local threats as soon as possible in order to improve the integrity of GNSS receivers.

DOI: 10.1134/S2075108717010035

I. INTRODUCTION

With the widespread deployment of Global Navigation Satellite Systems (GNSS) [1], one of the major challenges to be solved is the provision of integrity to users beyond the civil aviation community, where this feature is already a well-established performance criterion. Integrity refers to the ability of the user receiver to guarantee the quality and trust of the received signal, in such a way that critical or commercial applications can be safely operated.

Position integrity is typically provided in civil aviation by Receiver Autonomous Integrity Monitoring (RAIM) algorithms and Satellite Based Augmentation Systems (SBAS). However, such methods assume that local effects like multipath, Non-Line-Of-Sight (NLOS) propagation, radio frequency interference and spoofing have a controlled influence on the signal [2], which is not the case in terrestrial environments. This is the reason why the analysis of signal integrity greatly contributes to the capability to provide PVT integrity, which is currently a concern within the GNSS community.

In order to improve integrity in terrestrial environments we have to detect local effects as soon as possible with the aim of promptly alerting the user. So far, contributions have been addressed adopting a classical detection framework [3–5], which is not well suited to fulfill the requirements of safety-critical applications. Alternatives may be based on the use of bank of Kalman filters as used in the pioneering work [6] and in [7] or in the recent work [8]. Nevertheless, these methods have the drawback of a high computational complexity and they assume Gaussianity in the measurements. On the other hand, mitigation techniques have attracted the attention of many researchers during the past years [9–12], leaving the detection of these threats in a secondary place, when indeed it is even more important than mitigation, especially for NLOS. The reason is that before using mitigation techniques, we can benefit from knowing whether these threats are present or not. For instance we can discard the current measurements [13], thus not requiring complicated mitigation techniques, or apply mitigation as soon as possible.

For the prompt detection of integrity threats, it is essential to formulate the problem under the framework of statistical change detection, which is also often known as quickest detection. This framework is aimed at minimizing the detection delay, and then it is the right way for proceeding in the problem under consideration. The quickest detection framework has been extensively studied in the past decades, being applied to many fields [14–16]. One of the most popular techniques is the CUSUM algorithm, which was first proposed in 1954 by Page [17]. However, it was not until 1971 when Lorden [18] showed the optimality of the CUSUM from an asymptotic point of view (i.e. when the mean time between false alarms goes to infinity). And it was not until 1986 when Moustakides [19] proved the optimality of the CUSUM in a non-asymptotic framework. The long period between the CUSUM proposal by Page and the optimal results by Lorden and Moustakides makes evident the difficulties in analyzing the statistical properties and optimality theory of quickest detection.

As a matter of fact, there is scarce literature addressing the problem in a rigorous manner, being exceptions the work by Nikiforov [20] and Poor [21],

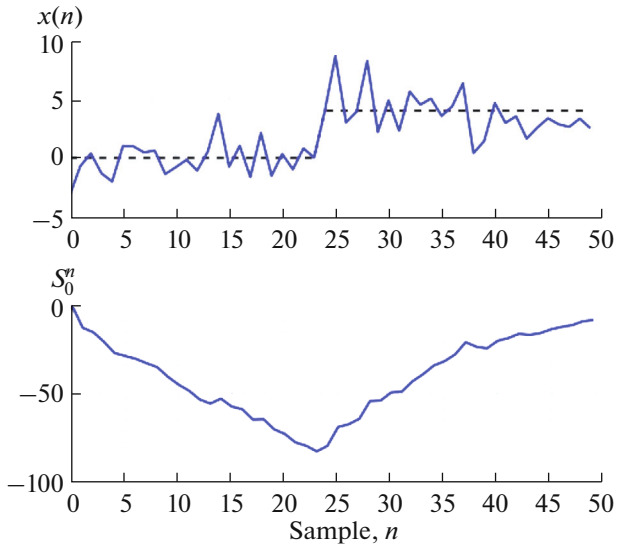

Fig. 1. Typical behavior of the cumulative LLR S_0^n (bottom plot) corresponding to a mean change ($\mu_0 = 0$ and $\mu_1 = 4$) of a Gaussian sequence with constant variance ($\sigma^2 = 2.5$) (upper plot), for $\nu = 25$.

which are not intended for a general reader. Based on this observation, the goal of this work is to provide a comprehensive analysis of the statistical properties of the CUSUM algorithm (optimality results are out of the scope of this work) and its application to local threat detection in GNSS. We already addressed this problem in [22]. In the present paper, though, we extend the work by giving a more detailed explanation in terms of different interpretations of the CUSUM (Sec. III-A) and demonstration of some key concepts (Sec. III-B). Moreover, we provide the proof of the results in Sec. III-C, which has not been presented so far. In essence, our main goal is to introduce and stimulate the use of quickest detection within the GNSS community, in particular, in those applications where threats must promptly be detected.

The rest of this paper is organized as follows. Section II introduces the signal model and Section III introduces the fundamentals of quickest detection. In Section IV we present the application of quickest detection to interference and multipath detection. Finally, Section V concludes the paper.

II. SIGNAL MODEL

Let us consider a sequence of independent observations $\{x(0), x(1), \ldots, x(\nu), x(\nu+1)\ldots\}$, with ν the time instant at which an integrity threat appears. Consequently, it is assumed that before $\nu(\mathcal{H}_0)$ the observation $x(n)$ follows a given statistical distribution, whereas after the change ($\mathcal{H}_1$) it follows a different one:

$$\begin{aligned} \mathcal{H}_0 &: x(n) \sim f_0(x(n)), \quad n < \nu \\ \mathcal{H}_1 &: x(n) \sim f_1(x(n)), \quad n \geq \nu. \end{aligned} \tag{1}$$

Based on these premises, quickest detection aims at finding the strategy that minimizes the detection delay, while keeping the mean time between false alarms larger than a conveniently set value. For this purpose, the CUSUM algorithm was proposed by Page [17] based on a key concept in statistics, namely the logarithm of the likelihood ratio or the log-likelihood ratio (LLR)

$$\mathrm{LLR}(n) \doteq \ln \frac{f_1(x(n))}{f_0(x(n))}. \tag{2}$$

A fundamental property of this ratio is as follows: Let E_0 and E_1 denote the expectations under the two distributions f_0 and f_1, respectively. Hence,

$$\mathrm{E}_0\,[\mathrm{LLR}(n)] < 0 \text{ and } \mathrm{E}_1\,[\mathrm{LLR}(n)] > 0, \tag{3}$$

namely, *a change in the distribution of the random variables x(n) is reflected as a change in the sign of the mean value of the log-likelihood ratio.* This is depicted in Fig. 1, which shows the cumulative LLR (lower plot),

$$S_0^n = \sum_{i=0}^{n} \mathrm{LLR}(i), \tag{4}$$

for the case of a Gaussian set of observations (upper plot) with mean before change $\mu_0 = 0$, mean after change $\mu_1 = 4$ and constant variance $\sigma^2 = 2.5$. The unknown change time is set to $\nu = 25$ samples.

In this case, the probability density functions (pdf) are

$$f_{0,1}(x) = \frac{1}{\sigma\sqrt{2\pi}} e^{-\frac{(x-\mu_{0,1})^2}{2\sigma^2}}, \tag{5}$$

and then

$$\mathrm{LLR}(n) = \frac{\mu_1 - \mu_0}{\sigma^2}\left(x(n) - \frac{\mu_1 - \mu_0}{2}\right), \tag{6}$$

with $\mu_{0,1}$ the mean value of the incoming observations before and after change, respectively. Therefore,

$$S_0^n = \frac{\mu_1 - \mu_0}{\sigma^2} \sum_{i=0}^{n} \left(x(i) - \frac{\mu_1 + \mu_0}{2}\right). \tag{7}$$

It is worth pointing out that these results are for the particular case of having a change in the mean of a Gaussian distribution. However, (3) holds true for any kind of change and thus any distributions f_0 and f_1. Moreover, we assume that both distributions are known. In practice, this is particularly true for f_0 because it models the nominal conditions, which are completely known. However, f_1 is usually unknown, rather some parameter of this distribution is unknown. In order to avoid nuisance parameters we fix the unknown parameters according to the minimum change we want to detect, so that the change will be

detected as long as the actual change is greater or equal than the fixed one.

III. FUNDAMENTALS OF QUICKEST DETECTION

In this section, we provide an overview of the most important theoretical results of quickest detection and it is aimed at introducing this theory to the GNSS community. We first introduce several derivations of the CUSUM algorithm in order to familiarize with the quickest detection problem. These derivations can be found in [20]. Secondly, we analyze the properties of the CUSUM algorithm, which are mainly stated in Theorems 1 and 2. These theorems can be found in [20] and [21]. Finally, we study the case when we have unknown parameters, suggesting an alternative to the CUSUM algorithm and analyzing its performance, stated in Theorem 3. To the best of the authors' knowledge, the proof of this theorem is something new.

A. CUSUM Derivation

Next, we introduce the CUSUM algorithm explaining different derivations of the algorithm.

INTUITIVE APPROACH

As it has been depicted in Fig. 1, the typical behavior of the cumulative LLR shows a negative drift before change and a positive drift afterwards. With this behavior, the relevant information lies in the difference between the value of the cumulative LLR and its current minimum value. Therefore, the corresponding decision rule is, at each instant, to compare this difference to a threshold h as

$$g(n) = S_0^n - m(n) \geq h, \tag{8}$$

with S_0^n as in (4) and

$$m(n) = \min_{1 \leq j \leq n} S_0^j. \tag{9}$$

PAGE'S APPROACH

The previous derivation of the CUSUM algorithm is a kind of intuition-based one. Next, we show the derivation of the CUSUM algorithm based upon a repeated use of the *sequential probability ratio test* (SPRT). Details on the SPRT can be found in [23]. The idea of Page [17] was to test the two simple hypotheses for successive values of n

$$\begin{aligned} \mathcal{H}_0 &: f(\mathbf{x}(n)) = f_0(\mathbf{x}(n)), \\ \mathcal{H}_1 &: f(\mathbf{x}(n)) = f_1(\mathbf{x}(n)), \end{aligned} \tag{10}$$

with the aid of the SPRT, where $\mathbf{x}(n)$ is defined as the vector that contains $x(0)$, $x(1)$, ..., $x(n)$ and $\{f_0(\mathbf{x}(n)), f_1(\mathbf{x}(n))\}$ the multivariate versions of $\{f_0(x(n)), f_1(x(n))\}$ in (1). The SPRT is defined by the pair (d, T), where d is a *terminal decision rule* taking values in the set $\{0, 1\}$, and T is a *stopping time* defined as the time at which the final decision is taken.

Thereby, T declares the time to stop sampling, and once the value of T is given, d takes the value 0 or 1 declaring which of the two hypotheses to accept (i.e. $\mathcal{H}_0$ or $\mathcal{H}_1$, respectively). Formally,

$$d = \begin{cases} 0, & \text{if} \quad S_0^T \leq -\epsilon \\ 1, & \text{if} \quad S_0^T \geq h, \end{cases} \tag{11}$$

where T is the stopping time defined as

$$T = T_{-\epsilon,h} \doteq \min\{n : (S_0^n \geq h) \cup (S_0^n \leq -\epsilon)\}. \tag{12}$$

The thresholds $\epsilon \geq 0$ and $h \geq 0$ are conveniently chosen according to some probability of false alarm (α) and some probability of missed detection (γ). Then, the key idea of Page was to *restart the SPRT algorithm whenever the taken decision was* $d = 0$. Moreover, the first time at which $d = 1$, the SPRT is stopped and this time becomes the *stopping time* or *alarm time* at which the change is detected. To do so, Page suggested that the optimal value of the lower threshold ϵ should be zero (i.e. $\epsilon = 0$) and thus, repeating the SPRT with this threshold, the resulting *decision rule* can be written as

$$g(n) = \begin{cases} g_{\mathrm{LLR}}(n), & \text{if} \quad g_{\mathrm{LLR}}(n) > 0, \\ 0, & \text{if} \quad g_{\mathrm{LLR}}(n) \leq 0 \end{cases} \tag{13}$$

with $g_{\mathrm{LLR}}(n) = g(n-1) + \mathrm{LLR}(n)$ and $g(0) = 0$. This decision rule can be compacted into

$$g(n) = (g(n-1) + \mathrm{LLR}(n))^+, \tag{14}$$

where $(x)^+ = \max(0, x)$. Thus, the stopping time is defined by the well-known expression for the CUSUM algorithm

$$t_a \doteq \min\{n : g(n) \geq h\}. \tag{15}$$

LORDEN'S APPROACH

Finally, let us introduce an idea due to Lorden [18] that turns out to be useful for analyzing change detectors. First, it is worth noting that (8) can be rewritten as

$$g(n) = \max_{1 \leq j \leq n} S_j^n, \tag{16}$$

with $S_j^n \doteq \sum_{i=j}^n \mathrm{LLR}(i)$. With this result in mind, the CUSUM stopping time t_a can be interpreted as a set of *parallel* so-called open-ended SPRT, which are activated at each possible change time $j = 1, ..., n$, and with upper threshold h and lower threshold $-\epsilon = -\infty$. Each of these SPRT stop at time n if, for some $j \leq n$, the observations $x_j, ..., x_n$ are significant for accepting the

change. This can be formalized as follows. Let T_j be the stopping time for the SPRT activated at time j

$$T_j = \min\{n \geq j : S_j^n \geq h\}, \tag{17}$$

with the convention that $T_j = \infty$ when this minimum is never reached. Let us now define the following stopping time as the minimum of the T_j

$$T^* \doteq \min_{j=1,2,\ldots}\{T_j\}. \tag{18}$$

Comparing (15) and (18), with the definition of $g(n)$ in (16), we see that $t_a = T^*$.

B. Properties of the CUSUM algorithm

In this section, we describe several criteria for the performance evaluation of the CUSUM algorithm with the aim of providing a way for setting the detection threshold h in order to obtain a desired performance. To assess the goodness of the resulting detector, it is convenient to use the mean delay for detection (i.e. $\overline{\tau} = \mathrm{E}_1[t_\alpha]$) and the mean time between false alarms (i.e. $\overline{T} = \mathrm{E}_0[t_\alpha]$). In fact, it would be interesting to have a specific function that contains all the information related to both values. This function is the average run length (ARL), defined as

$$L_\theta(\mathcal{T}) \doteq \mathrm{E}_\theta[\mathcal{T}], \tag{19}$$

where $\theta = \theta_0$ under $\mathcal{H}_0$ and $\theta = \theta_1$ under $\mathcal{H}_1$, and $\mathcal{T}$ is the stopping time. Thereby, the ARL function defines at θ_0 the mean time between false alarms, and at θ_1 the mean delay for detection.

Let us now define two important concepts useful for the analysis of the statistical properties of the SPRT and that will be used for the computation of the ARL of the CUSUM algorithm. Such a computation of the ARL appears in [20] and [21] and is presented in Theorem 1.

Definition 1 (ASN). *The* average sample number (*ASN*) *of a SPRT is the mean number of samples* $\mathrm{E}_\theta[T_{-\epsilon,h}]$ *necessary for testing the hypotheses with acceptable conditions (i.e.* α *and* γ*).*

Definition 2 (OC). *The probability* $\mathrm{P}_\theta\,(T_{-\epsilon,\ h})$ *of accepting hypothesis* H_0 (*i.e. the SPRT reaches the lower threshold* $-\epsilon$) *is called the* operating characteristic (OC).

Theorem 1. *If* $\mathrm{E}_\theta[T_{0,\ h}]$ *and* $\mathrm{P}_\theta\,(T_0,\ h)$ *are the ASN and* OC*, respectively, of a SPRT with thresholds* $-\epsilon = 0$ *and h, the ARL for the CUSUM algorithm* $L_\theta(t_a)$ *is*

$$L_\theta(t_a) = \mathrm{E}_\theta[t_a] = \frac{\mathrm{E}_\theta[T_{0,h}]}{1 - \mathrm{P}_\theta[T_{0,h}]}. \tag{20}$$

Proof: Taking into account that the CUSUM algorithm can be derived with the aid of a SPRT formulation, it is possible to link the ARL function of the CUSUM algorithm with the statistical properties of the SPRT with lower threshold $\epsilon = 0$ and upper threshold h. With this formulation it is possible to write the ARL function as

$$\begin{aligned} L_\theta(t_a) = \mathrm{E}_\theta[t_a] = \mathrm{E}_\theta\left[T_{-\epsilon,h}\middle| S_0^{T_{-\epsilon,h}} \leq -\epsilon\right]\cdot \mathrm{E}_\theta[c-1] \\ + \mathrm{E}_\theta\left[T_{-\epsilon,h}\middle| S_0^{T_{-\epsilon,h}} \geq h\right]\cdot 1, \end{aligned} \tag{21}$$

where $\mathrm{E}_\theta[T_{-\epsilon,\ h}|S_0^{T_{-\epsilon,h}} \leq -\epsilon]$ is the conditional ASN of one cycle of SPRT when the cumulative sum reaches the lower threshold $-\epsilon$, and $\mathrm{E}_\theta[T_{-\epsilon,\ h}|S_0^{T_{-\epsilon,h}} \geq h]$ is the conditional ASN of one cycle of SPRT when the cumulative sum reaches the upper threshold h, and then a final decision is taken.

In (21), $\mathrm{E}_\theta[c-1]$ is the mean number of cycles before the cycle of final decision (i.e. before the cumulative sum reaches the upper threshold *h)*. The random variable $y = c - 1$ can be represented as a geometrical random variable with distribution $f(y) = (1-p)p^y$ for $y = 0,1,2,\ldots$, where $p = \mathrm{P}_\theta\,(T_{-\epsilon,\ h})$ is the OC. Thus,

$$\mathrm{E}_\theta[c-1] = \frac{p}{1-p}, \tag{22}$$

and it results from (21) that

$$\begin{aligned} L_\theta(t_a) = \frac{\mathrm{E}_\theta\left[T_{-\epsilon,h}\middle| S_0^{T_{-\epsilon,h}} \leq -\epsilon\right]p}{1-p} \\ + \frac{\mathrm{E}_\theta\left[T_{-\epsilon,h}\middle| S_0^{T_{-\epsilon,h}} \geq h\right](1-p)}{1-p}. \end{aligned} \tag{23}$$

Now, considering that p is the OC of the stopping time $T_{-\epsilon,\ h}$, we have that the summation of the two numerators in (23) is equal to $\mathrm{E}_\theta[T_{-\epsilon,\ h}]$. Therefore, with these considerations and using the value of the lower threshold for the CUSUM (i.e. $\epsilon = 0$) the result in (20) follows.

The ASN and OC are solutions of the Fredholm integral equation of the second kind, which has to be solved numerically. In order to avoid this numerical solution, and with the aim of making easier the design of the CUSUM algorithm, some approximations are available [20]. Usually, bounds on the ARL function are more desirable than approximations. This is because, in practice, it is important to fix a conveniently chosen performance of the change detection algorithm (given by the fixed threshold h) and then be sure that this performance will always be achieved within some limits. This is particularly important for online integrity monitoring, where the working conditions vary along time and then the threshold h should be computed continuously, as well. For this purpose, the use of bounds is mandatory to ensure that the desirable limits are always preserved.

Theorem 2. *If* $\mathrm{K}(f_1, f_0) \doteq \mathrm{E}_1[\mathrm{LLR}(n)]$ *is the Kullback-Leibler divergence between* f_1 *and* f_0*, the bounds for the mean time between false alarms and the detection delay of the CUSUM algorithm are*

$$\begin{aligned} \bar{T} &\geq e^{h}, \\ \bar{\tau} &\leq \frac{h}{K(f_1, f_0)}. \end{aligned} \tag{24}$$

Proof: A lower bound for $\bar{T}$ can be obtained from Wald's inequalities [23]

$$h \leq \ln\left(\frac{1-\gamma}{\alpha}\right) \quad \text{and} \quad -\epsilon \geq \ln\left(\frac{\gamma}{1-\alpha}\right), \tag{25}$$

with γ and α the probability of missed detection and false alarm, respectively, of the SPRT. For the CUSUM algorithm the lower threshold is equal to zero (i.e. $\epsilon = 0$). Regarding the missed detection probability, *the CUSUM algorithm will always detect the presence of a change. It would take more or less time, but it will detect the change. Therefore the missed detection probability of the CUSUM detection is equal to zero (i.e.,* $\gamma = 0$) and, from (25), $h \leq -\ln(\alpha)$. With these considerations, taking into account that the mean time between false alarms can be defined as the inverse of the false alarm rate (i.e. $\bar{T} = 1/\alpha$*),* the lower bound for $\bar{T}$ in (24) follows.

On the other hand, we can obtain an upper bound for the mean detection delay from the result of the Wald's approximations [23]:

$$\bar{\tau} = \mathrm{E}_1[t_a] \approx \mathrm{K}(f_1, f_0)^{-1} \times ((1-\gamma)h - \gamma\epsilon), \tag{26}$$

with $\mathrm{K}(f_1, f_0) \doteq \mathrm{E}_1[\mathrm{LLR}(n)]$ the Kullback–Leibler divergence between f_1 and f_0. Taking into account the previous considerations and the Wald's inequalities, the upper bound for the detection delay in (24) follows.

A similar proof of Theorem 2 can be found in [21]. Results in (24) provide us the asymptotic (i.e. when h goes to infinity) relationship between the mean time between false alarms and the detection delay with the fixed threshold. These results have been proved to be the optimal ones for the quickest detection problem. As we have already commented, Lorden [18] showed that the CUSUM procedure *asymptotically* minimizes the detection delay, attaining the bounds in (24). Lorden's method is based on linking the CUSUM algorithm with the SPRT, similarly as we do in this section. On the other hand, instead of studying the optimal detection problem via SPRT, Moustakides [19] was able to formulate the problem as an optimal stopping problem and to prove that the CUSUM rule is indeed the optimal solution.

In some sense, results in (24) play the same role in the change detection theory as the Cramer–Rao lower bound in estimation theory, or as the receiver operating characteristic (ROC) in classical detection. It is worth mentioning that the optimal results are obtained when the CUSUM algorithm is tuned with the true values of the distributions before and after the change. When the algorithm is used in situations where the actual distribution is different from the assumed ones, this optimal property cannot be guaranteed anymore.

C. Unknown Log Likelihood Ratio

In this section, we discuss the case when the LLR is not completely known, that is the case when the parameters under $\mathcal{H}_1$ are unknown. Without loss of generality, the parameters under $\mathcal{H}_0$ are assumed to be known. Thus, two possible solutions exist [20]:

- **Weighted Likelihood Ratio (WLR)**: To weight the likelihood ratio with respect to all possible values of the parameters under $\mathcal{H}_1$ (i.e. θ_1), using a weighting function $dF(\theta_1)$ dependent on the probability of occurrence of θ_1.

$$\tilde{\Lambda}(n) \doteq \int_{-\infty}^{\infty} \frac{f_1(x(n))}{f_0(x(n))} dF(\theta_1). \tag{27}$$

- **Generalized Likelihood Ratio (GLR)**: To replace the unknown parameters θ_1 by its maximum likelihood estimate.

$$\tilde{\Lambda}(n) \doteq \frac{\sup_{\theta_1} f_1(x(n); \theta_1)}{f_0(x(n))}. \tag{28}$$

In other words, for known θ_1, change detection algorithms are based on the likelihood ratio $\Lambda(n) \doteq f_1(x(n))/f_0(x(n))$. For unknown θ_1, $\Lambda(n)$ must be replaced by other statistic like $\tilde{\Lambda}(n)$ or $\hat{\Lambda}(n)$. Nonetheless, for the WLR we need information about the unknown parameters, which is not a common situation. On the other hand, in general, the GLR-CUSUM cannot be written in a recursive form since it depends upon the maximization over the unknown time change (i.e. we need all the collected samples). This gives rise to a big computational burden. It is for these reasons that we propose an alternative CUSUM-based approach (i.e. offset-CUSUM) in order to avoid the previous practical issues.

Thus, in general, when the LLR is not completely known, it can be replaced by any other function of the observations $x(n)$. That is to say, $\rho(n) \doteq q(x(n))$ with negative mean before the change and positive mean after the change (i.e. $\mathrm{E}_0[\rho(n)] < 0$ and $\mathrm{E}_1[\rho(n)] > 0$), in line with the key idea of the CUSUM (see (3)). That is,

$$g_{\mathrm{offset}}(n) \doteq g_{\mathrm{offset}}(n-1) + \rho(n))^{+}. \tag{29}$$

And then, the stopping time is defined by

$$\tilde{t} \doteq \min\{n : g_{\mathrm{offset}}(n) \geq h\}. \tag{30}$$

In this case, the detection rule is no longer guaranteed to be optimal. Nevertheless, it is still a very good candidate, provided that an appropriate function $\rho(n)$ is chosen.

Theorem 3. *If* $\omega_0 > 0$ *is the nonzero root of the equation* $\mathrm{E}_0[e^{\omega\rho(n)}] = 1$, *the bounds for the mean time between false alarms and the detection delay of the offset-CUSUM are given by the following expressions*

$$\begin{aligned} \overline{T} &\geq e^{\omega_0 h}, \\ \overline{\tau} &\leq \frac{h}{\mathrm{E}_1[\rho(n)]}. \end{aligned} \tag{31}$$

Proof: The proof is found in the Appendix.

The proof of Theorem 3 is based on results in [20], but to the best of the authors' knowledge it is a new contribution. Usually, the mean before the change of $\rho(n)$ is not negative and then the idea proposed above is not applicable. In that case, we propose the modified metric

$$\rho(n) \doteq \rho_b(n) - b, \tag{32}$$

and then, by selecting a proper offset b, the mean of $\rho(n)$ before the change will be negative, but it will become positive after the change. Specifically, the choice of the offset b should be large enough to ensure a negative mean before change and to provide a certain false alarm rate. But at the same time, b should be small enough to maintain a positive mean after change. From (31) and using expression of $\rho(n)$ in (32), we are able to adjust the false alarm rate through the nonzero root, ω_0, of the following equation

$$\mathrm{E}_0[e^{\omega(\rho_b(n)-b)}] = \mathrm{E}_0[e^{\omega\rho_b(n)}]e^{-\omega b} = 1, \tag{33}$$

where $\mathrm{E}_0[e^{\omega\rho_b(n)}]$ is the characteristic function of $\rho_b(n)$ under $\mathcal{H}_0$.

IV. QUICKEST DETECTION FOR INTEGRITY MONITORING

This section describes the application of the CUSUM algorithm to GNSS integrity monitoring. To do so, we use the CUSUM algorithm for interference and multipath detection, which are the most relevant and common problems in GNSS. We show different situations for applying the CUSUM algorithm in order to be used as a guideline for further works in GNSS integrity. Some results using real GNSS receiver data are shown. For a more extensive analysis with real signal confirming the models and theoretical results presented in this section see [24] and [25]. Also, it is worth pointing out that we assume temporal statistical independence of the metrics used at the input of the CUSUM algorithm. This is a fair assumption since the metrics are computed using disjoint blocks of data whose length is typically much larger than the coherence time of the disturbing effect.

A. CASE 1 (Interference): Completely Known LLR

This section presents the case when both distributions before and after the change are completely known. This situation is often the case when addressing interference detection in GNSS. Interference detection must be carried out at the output of the GNSS front-end, since it is here where the interference is visible (i.e. before de-spreading). In the absence of interference, the received signal will be dominated by noise, since the GNSS signal remains under the noise floor, whereas in the presence of interference the received signal will be dominated by the interference itself due to the high interference power.

The detection problem thus becomes:

$$\begin{aligned} \mathcal{H}_0 &: r(n) = w(n), \quad n < \nu \\ \mathcal{H}_1 &: r(n) = i(n) + w(n), \quad n \geq \nu, \end{aligned} \tag{34}$$

where $r(n)$ represents the discrete-time base-band sample at time n, $i(n)$ models the interference signal impinging into the GNSS receiver, and $w(n)$ is the thermal noise disturbing the received samples, which can be modeled as an independent and identically distributed (i.i.d.) zero-mean Gaussian random process. Next, we propose a detection method based on the statistical analysis of the received data. That is, it is based on the fact that, in the absence of interference, the samples at the front-end output should follow a Gaussian distribution.

The kurtosis value is a good metric for measuring the Gaussianity of the data. It is a statistical measurement equal to 3 if the data is Gaussian (i.e. under $\mathcal{H}_0$), otherwise (i.e. under $\mathcal{H}_1$) it departs from 3. Let us define the kurtosis estimate as

$$\hat{R}(m) \doteq \frac{\hat{\zeta}_4^{(m)}}{\hat{\zeta}_2^{(m)^2}}, \tag{35}$$

with $\hat{\zeta}_i^{(m)}$ the N-samples estimates of the i-th central moment of $r(n)$. In turn, m stands for the snapshot index, where each snapshot includes N samples.

In [26] it is stated that for large N (i.e. $N \gg 1000$), the estimate of the kurtosis of a Gaussian variable is another Gaussian variable with mean and variance below,

$$\begin{aligned} \mathrm{E}_0[\hat{R}(m)] &= \mu_0^{(\mathrm{k})} = 3\frac{N-1}{N+1}, \\ \mathrm{var}_0[\hat{R}(m)] &= \sigma_0^{2^{(\mathrm{k})}} = \frac{24}{N}. \end{aligned} \tag{36}$$

Moreover, in the presence of interference, the kurtosis estimates are still Gaussian distributed but suffering from a change in both mean and variance. From [27] we have the following expression for the mean after change

$$\mathrm{E}_1[\hat{R}(m)] = \mu_1^{(\mathrm{k})} = \mu_0^{(\mathrm{k})} \frac{1 + 2\mathrm{INR} + \frac{\mathrm{INR}^2}{2k}}{(1+\mathrm{INR})^2}, \tag{37}$$

where INR is the interference-to-noise ratio, and $0 < \kappa < 1$ the duty cycle. This is so for any kind of interfer-

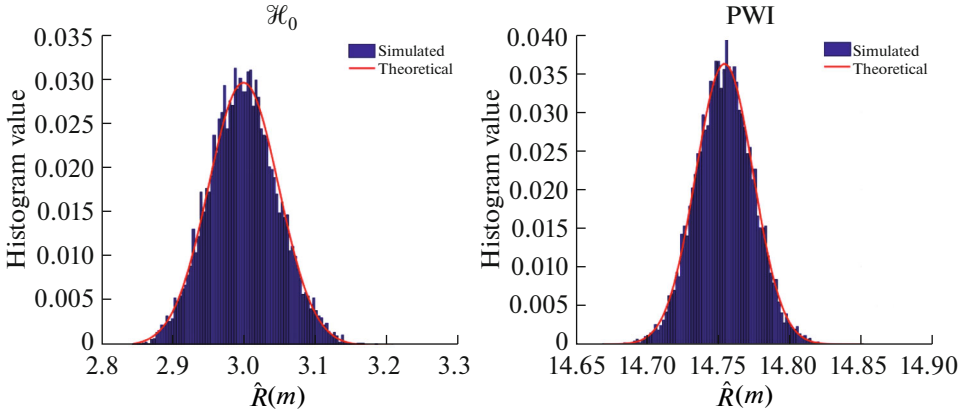

Fig. 2. Statistical characterization of the kurtosis value. Comparison between simulated (i.e. histogram) and theoretical distribution under $\mathcal{H}_0$ (left) and $\mathcal{H}_1$ with a pulsed wave interference (right).

ence, both pulsed and continuous (i.e. $\kappa = 1$), except for wide-band ones, which maintain the Gaussianity of the data and then the kurtosis value does not vary.

Thereby, we can formulate the kurtosis-based detection in a quickest interference detection framework as

$$\begin{aligned} \mathcal{H}_0 &: \hat{R}(m) \sim N(\mu_0^{(k)}, \sigma_0^{2^{(k)}}), \quad m < \nu \\ \mathcal{H}_1 &: \hat{R}(m) \sim N(\mu_1^{(k)}, \sigma_1^{2^{(k)}}). \quad m \geq \nu. \end{aligned} \tag{38}$$

This is shown in Fig. 2, which presents the distribution of the kurtosis for the case of nominal conditions and under the presence of a pulsed wave interference (PW). We see how under $\mathcal{H}_0$ (see left plot) the kurtosis distribution is Gaussian with a mean close to 3. On the other hand, under $\mathcal{H}_1$ (see right plot) the kurtosis distribution is still Gaussian but the mean departs from the baseline value equal to 3. These results have been obtained with $N = 10^4$ samples, INR = 20 dB, a PW with $\kappa = 0.1$, and 10^5 Monte-Carlo runs. This value of INR is selected to show a distinguishable change in the mean of the kurtosis.

From (38) we have characterized the statistical behavior of the kurtosis, with $\mu_0^{(k)}$, $2\sigma_0^{2^{(k)}}$ and $\mu_1^{(k)}$ known. However, $\sigma_1^{2^{(k)}}$ is typically unknown, and then we cannot fully characterize the distribution under $\mathcal{H}_1$. Nevertheless, we can assume that both variances before and after the change are equal (i.e. $\sigma_0^{2^{(k)}} = \sigma_1^{2^{(k)}}$), and then use the CUSUM algorithm as a Gaussian mean change detector. Doing so, we are able to express the LLR as

$$\mathrm{LLR}_k(m) = \frac{\mu_1^{(k)} - \mu_0^{(k)}}{\sigma_0^{2^{(k)}}} \left(\hat{R}(m) - \frac{\mu_1^{(k)} + \mu_0^{(k)}}{2} \right), \tag{39}$$

with $\mu_0^{(k)}$, $\sigma_0^{2^{(k)}}$ and $\mu_1^{(k)}$ defined as in (36)–(37), and $\hat{R}(m)$ the N-sample kurtosis estimate at snapshot m.

It is worth noting that $\mu_1^{(k)}$ is known to depend on the INR and the duty cycle of the interference. Hence, a way to proceed is to fix a certain value for $\mu_1^{(k)}$ according to the minimum INR that one expects to detect. Moreover, the duty cycle might be fixed to the value that produces the minimum change possible. In this way, a minimum change detection is set allowing the detection of any larger change caused by higher power interferences or with duty cycle that give rise to larger changes in the kurtosis. Thus, we can make use of the CUSUM algorithm decision rule as

$$g^{(k)}(m) = (g^{(k)}(m-1) + \mathrm{LLR}_k(m))^+ \geq h_k, \tag{40}$$

leading to the following performance

$$\begin{aligned} \overline{T}_{\mathrm{kurt}} &\geq e^{h_k}, \\ \overline{\tau}_{\mathrm{kurt}} &\leq \frac{h_k}{\mathrm{K}_k(f_1, f_0)}, \end{aligned} \tag{41}$$

with $\mathrm{K}_k(f_1, f_0) = (\mu_1^{(k)} - (\mu_0^{(k)})^2/(2\sigma_0^{2^{(k)}})$.

These bounds are presented in Fig. 3, which are compared with simulated results. We use $N = 10^4$ and 10^5 Mote-Carlo runs. In addition, for the detection delay case we fix INR = −10 dB. This low value is selected in order to show representative results, otherwise the detection delay would be just one sample. The left plot shows that the simulated number of samples between false alarms is larger than the lower bound, which allows us to set a threshold h_k assuring certain desired false alarm rate. Moreover, the right plot shows similar values for the simulated and theoretical results on detection delay.

B. CASE 2 (Interference): Unknown LLR

Here, we present the case when the distribution after the change is completely unknown. To do so, we apply the CUSUM algorithm to interference detection

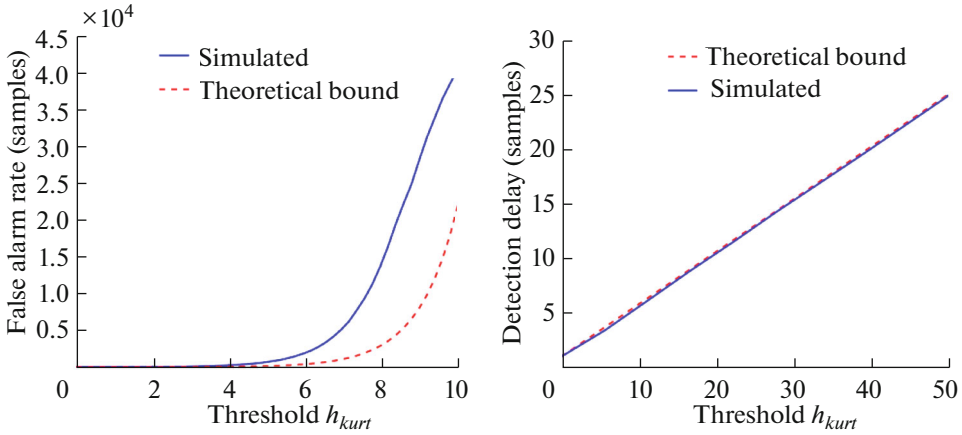

Fig. 3. CUSUM performance for the kurtosis method with respect to the detection threshold and $N = 10^4$. False alarm rate in samples (left) and detection delay for a PW with INR = −10 dB (right).

again, but using a different metric for measuring the Gaussianity of the received signal samples.

We know from (34) that in the interference free-case, the received signal is dominated by noise, so that the histogram of the received samples should follow a Gaussian shape. Meanwhile, when interference is present, the received signal is dominated by the interference , and then the histogram of the received samples should not follow a Gaussian shape. This detection problem is equivalent to a goodness-of-fit test (GoF), specifically, we are interested in determining whether our received signal follows a Gaussian distribution or not. To do so, we make use of the chi-square test, which uses a metric based on the histogram and have a known distribution under $\mathcal{H}_0$.

The chi-square test evaluates the next test statistic [26]

$$x_{\text{hist}}(m) = \sum_{i=1}^{N_b} \frac{(O_i^{(m)} - E_i)^2}{E_i}, \tag{42}$$

with E_i the value of the i-th bin of the reference *theoretical* histogram evaluated under $\mathcal{H}_0$ with N_b bins. These values are obtained by calculating the theoretical pdf for each bin and transforming it to a histogram value (i.e. taking into account the snapshot samples N and the separation between bins). $O_i^{(m)}$ is the value of the i-th bin of the measured histogram with N_b bins at snapshot m, where each snapshot contains N samples.

Pearson [26] claimed that for large N, the variable $x_{\text{hist}}(m)$ under $\mathcal{H}_0$ is approximately chi-squared distributed with N_b — 1 degrees of freedom, whereas under $\mathcal{H}_1$ it departs from a central chi-square distribution. Therefore, we can write the following hypotheses

$$\begin{aligned} \mathcal{H}_0 &: x_{\text{hist}}(m) \sim \chi^2(N_b - 1), \quad m < \nu \\ \mathcal{H}_1 &: x_{\text{hist}}(m) \not\sim \chi^2(N_b - 1), \quad m \geq \nu. \end{aligned} \tag{43}$$

This is depicted in Fig. 4. We can see how under $\mathcal{H}_0$ (see left plot) the histogram of the simulated data almost fits the theoretical χ^2 with $N_b - 1$ degrees of freedom. On the other hand, in the right plot, the histogram is shown for the case when the simulated interference is present. It can be seen how it departs from the $\chi^2(N_b - 1)$ distribution, which is expected under $\mathcal{H}_0$. The results have been obtained using a number of $N = 10^4$ samples, 10^5 Monte-Carlo runs, a number of bins $N_b = 50$, and a continuous wave (CW) with INR = 20 dB for the $\mathcal{H}_1$ case. Again, this INR value is selected in order to show a visible change on distribution.

So far, we have seen that the pdf after change is different to that before the change, but we have no knowledge about this pdf. Hence, since the pdf under $\mathcal{H}_1$ is unknown, the LLR cannot be completely defined, and then we are unable to apply the CUSUM algorithm directly to $x_{\text{hist}}(m)$. However, since $\mathcal{H}_0$ is known, we can use the offset-CUSUM (Sec. III-C). To do so we need to propose a metric ρ that has a negative and positive mean before and after the change, respectively.

It is known that the mean of a χ^2 random variable is equal to the number of degrees of freedom of the χ^2. Therefore, E0 [xhist(m)] = Nb − 1 > 0. Hence, we cannot use directly $x_{\text{hist}}(m)$ as the function ρ, but we define the following modified function

$$\rho_{\text{hist}}(m) \doteq x_{\text{hist}}(m) - b, \tag{44}$$

with b a proper offset for which the mean of $\rho_{\text{hist}}(m)$ before change is negative, but it is positive after change.

Moreover, the choice of the offset b should be large enough to ensure a negative mean before change and to provide a certain false alarm rate, always maintain-

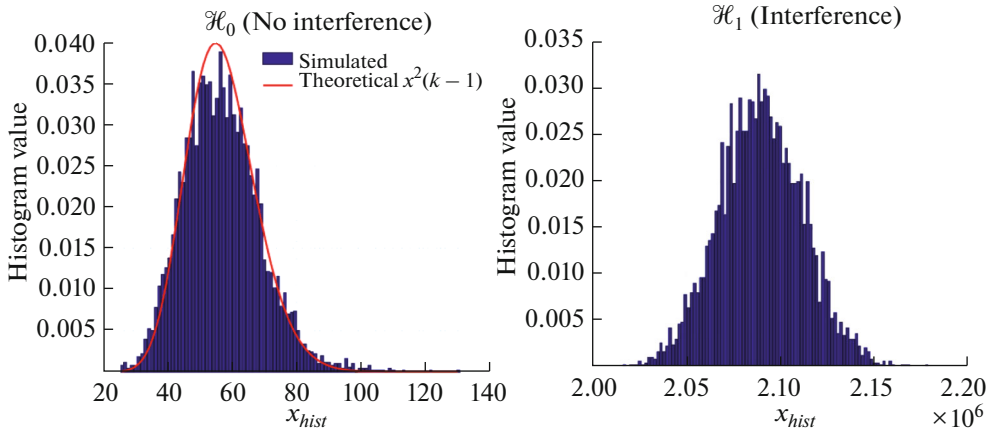

Fig. 4. Statistical characterization of the chi-squared GoF test metric. Comparison between simulated (i.e. histogram) an

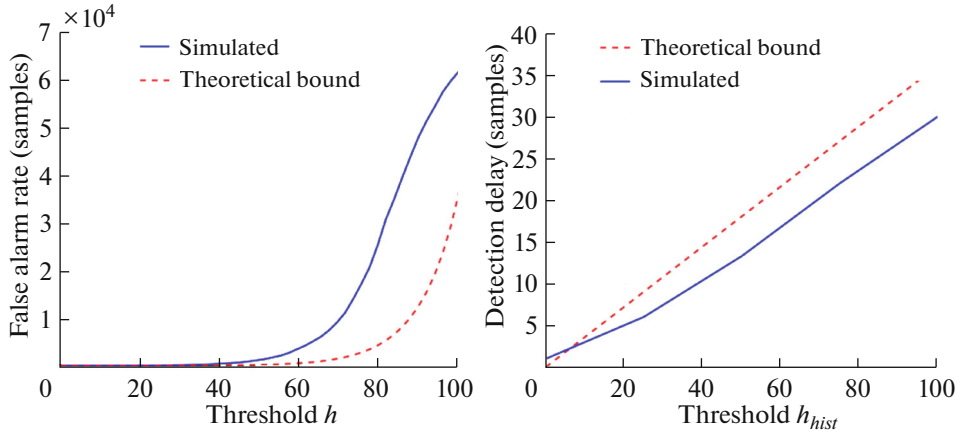

Fig. 5. Offset-CUSUM performance for the GoF metric as a function of detection threshold, with a fixed $N_b = 50$ and $b = 55$. False alarm rate (left) and detection delay for a CW with INR = −20 dB (right).

ing a positive mean after change. From (33) and using $\rho_{\text{hist}}(m)$ we are able to adjust the false alarm rate through the nonzero root ω_0 with (31), which turns out to be the nonzero root of the next equation

$$e^{\omega b} = (1 - 2\omega)^{-\frac{N_b - 1}{2}}, \tag{45}$$

which can be solved numerically. Thus, the choice of b will fix a value for ω_0 given by the equation above. Thereby, making use of the following decision rule

$$g^{(\text{hist})}_{\text{Offset}}(m) = \left(g^{(\text{hist})}_{\text{Offset}}(m-1) + \rho_{\text{hist}}(m)\right)^+ \geq h_{\text{hist}}, \tag{46}$$

we obtain the following performance

$$\begin{aligned} \overline{T}_{\text{hist}} &\geq e^{\omega_0 h_{\text{hist}}}, \\ \overline{\tau}_{\text{hist}} &\leq \frac{h_{\text{hist}}}{\mathrm{E}_1[\rho_{\text{hist}}(m)]}, \end{aligned} \tag{47}$$

where ω_0 is the nonzero solution of (45).

These bounds are proved in Fig. 5, which shows the offset-CUSUM performance using $\rho_{\text{hist}}(m)$, and compares it with the theoretical bounds above. We set the offset to $b = 55$, the number of bins to $N_b = 50$ and for the case of the detection delay we simulate a CW with INR = −20 dB. Again, this low value is chosen in order to show representative results. The left plot of Fig. 5 shows how the simulated number of samples between false alarms is greater than the lower bound given in (47). In addition, the right plot shows the detection delay measured in samples with respect to the set threshold, and shows similar values for the simulated results and theoretical ones, being the simulated delay below the upper bound given in (47).

C. CASE 3 (Multipath): Incompletely Known LLR

We present here the case when both the distribution before and after the change are known, but some of the parameters of them are unknown. This situation

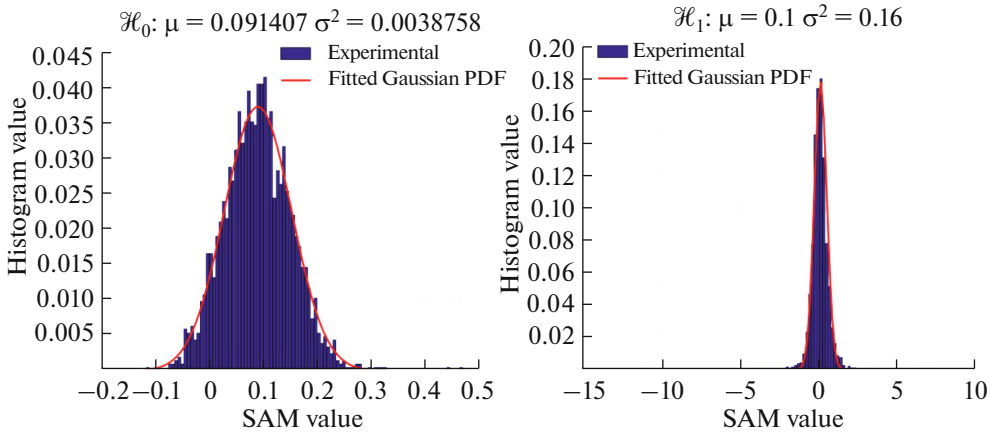

Fig. 6. Statistical characterization of SAM with real data captured in London downtown under benign conditions (left) and under harsh conditions (right).

is often the case when addressing multipath detection in GNSS. The problem of multipath detection in GNSS must be carried out at the acquisition and/or tracking stage, since it is there where multipath effects are visible (i.e. after de-spreading). Multipath affects tracking measures as the estimated C/N_0, the code discriminator output (DLL) and the shape of the correlation curve [28]. Therefore, we will able to detect NLOS and multipath based on the fluctuations of these measurements.

Now, we apply the CUSUM algorithm for the slope asymmetry metric (SAM), which is based on the correlation curves calculated in the tracking loop of any GNSS receiver [28]. We know that under benign conditions (i.e. $\mathcal{H}_0$) the correlation curve is symmetrical, but it loses the symmetry under harsh conditions (i.e. $\mathcal{H}_1$) due to the multipath components. This can be measured by the SAM, which under $\mathcal{H}_0$ is close to zero, indicating symmetry, whereas under $\mathcal{H}_1$ it departs from zero, indicating asymmetry. Specifically, when multipath is present we experience two different effects:

• Under LOS condition, the mean of the SAM departs from 0.

• Under NLOS condition, the variance of the SAM fluctuates.

Indeed, in both LOS and NLOS cases the mean and variance vary, but the mean change is predominant in LOS situations (i.e. deterministic component of LOS prevails), whereas the variance change is predominant in NLOS (i.e. random components due to multipath prevails). Therefore, this is equivalent to have a change on both the variance and mean of the SAM. Since the SAM is calculated from the Least Squares estimation of the slope at both sides of the correlation curve, we can assume that the distribution of the SAM is Gaussian, and then we can formulate the problem of multipath detection in a quickest detection framework as

$$\begin{aligned} \mathcal{H}_0 &: x_S(k) \sim N(\mu_0^{(S)}, \sigma_0^{2^{(S)}}), \quad k < \nu \\ \mathcal{H}_1 &: x_S(k) \sim N(\mu_1^{(S)}, \sigma_1^{2^{(S)}}), \quad k \geq \nu. \end{aligned} \tag{48}$$

This is presented in Fig. 6, which shows the histogram of the SAM values for data gathered with a real GNSS receiver in urban environment under the framework of the Integrity GNSS Receiver (iGNSSrx) project, funded by the European Commission. This data was captured during 80 s in a scenario (i.e., London downtown) that was under benign conditions the first 40 s, and then it changed to harsh conditions until the end of the captured data. We discriminate between benign and harsh conditions by analyzing the positioning error (i.e. using a truth reference). For the data under benign conditions we obtain a mean positioning error of 2 meters, whereas for the data under harsh conditions we obtain a mean positioning error of 50 meters.

In the left plot of Fig. 6 we present the histogram under benign conditions, where we see the Gaussianity of the SAM with a mean about 0.1. This value is due to the asymmetry introduced by the front-end filter and can be calibrated. On the other hand, in the right plot, we present the histogram under harsh conditions. We see how the histogram fits a Gaussian distribution quite well. This distribution has a mean that is also close to 0, but a much greater variance than under $\mathcal{H}_0$. This may be because in this case we are under NLOS conditions, and then the change on the variance is predominant.

We see that the SAM follows a Gaussian distribution with known mean before change (i.e. it must be calibrated) but unknown a-priori variance before and after the change. In order to use the CUSUM algorithm we propose the following configuration of the Gaussian distribution parameters:

• $\mu_0^{(S)}$: It should be equal to 0, but in practice it is slightly larger due to the shape of the front-end filter. Hence

$$\mu_0^{(S)} = \zeta \sim 0, \tag{49}$$

with $\zeta = 0.1$ herein.

• $\sigma_0^{2^{(S)}}$: This value is unknown a-priori because it is difficult to have a perfect knowledge of the actual variance, even knowing the expression for the variance of the SAM. This is so because it ultimately will depend on the multipath parameters, which will be random and unknown. Hence, we propose to fix the variance under benign conditions according to the *maximum* allowable variations on the SAM values under $\mathcal{H}_0$, as follows

$$\sigma_0^{2^{(S)}} \doteq \left(\frac{(\Delta_0)_{\max}}{3}\right)^2, \tag{50}$$

with $(\Delta_0)_{\max}$ the maximum allowable variations under $\mathcal{H}_0$. This is so because we know that for a Gaussian distribution the 99.86% of the values are comprised in the interval $\mu \pm 3\sigma$. For example, in our case we see that the SAM under $\mathcal{H}_0$ takes variations between -0.1–0.45. Therefore, a proper value for $(\Delta_0)_{\max}$ may be ± 0.4, which gives rise to $\sigma_0 = 1.78 \times 10^{-2}$.

• $\mu_1^{\pm(S)}$: This value is unknown, but it might be fixed as follow

$$\mu_1^{\pm(S)} = \mu_0^{(S)} \pm \delta, \tag{51}$$

with δ a proper value selected experimentally.

• $\sigma_1^{2^{(S)}}$: Similarly as for the variance before change, we fix the variance under harsh conditions as the *minimum* detectable variability on the SAM due to multipath as follows

$$\sigma_0^{2^{(S)}} \doteq \left(\frac{(\Delta_1)_{\min}}{3}\right)^2, \tag{52}$$

with $(\Delta_1)_{\min}$ the minimum detectable variation on the SAM under $\mathcal{H}_1$. For instance, in our case, a suitable value might be a variation equivalent to ± 0.6, which results in $\sigma_1^{2^{(S)}} = 4 \times 10^{-2}$.

Therefore, since the SAM may present a change in both mean and variance, we suggest the use of two different CUSUM algorithms, one for detecting the change in variance (i.e. NLOS) and another for detecting the mean change (i.e. LOS). The expression for the mean change CUSUM would be like (39), but with the SAM parameters. For the variance change CUSUM the LLR expression is as

$$\begin{aligned} \mathrm{LLR}_S(k) &= \ln\left(\frac{\sigma_0^{(S)}}{\sigma_1^{(S)}}\right) \\ &+ \frac{(x_S(k) - \mu_0^{(S)})^2}{2\sigma_0^{2^{(S)}}} - \frac{(x_S(k) - \mu_1^{(S)})^2}{2\sigma_1^{2^{(S)}}}, \end{aligned} \tag{53}$$

with $\mu_0^{(S)}$, $\sigma_0^{(S)}$, $\sigma_1^{(S)}$ defined as in (49)–(52), and $x_S(k)$ the calculated SAM value at the k-th post-correlation snapshot.

Thereby, we can use the following decision rule:

$$g^{(S)}(k) = (g^{(S)}(k-1) + \mathrm{LLR}_S(k))^+ \geq h_S, \tag{54}$$

leading to the next performance

$$\begin{aligned} \overline{T}_S &\geq e^{h_S}, \\ \overline{\tau}_S &\leq \frac{h_S}{\mathrm{K}_S(f_1, f_0)}, \end{aligned} \tag{55}$$

with $\mathrm{K}_S(f_1, f_0) = \ln(\sigma_0^{(S)}/\sigma_1^{(S)} + (\sigma_0^{2^{(S)}}/\sigma_1^{2^{(S)}}) - 0.5$.

In Fig. 7, we show the obtained SAM and the CUSUM evolution for the real data characterized in Fig. 6. We see in the left plot how the SAM presents a change in variance just when multipath appears (i.e., second 40). The change of the variance is quite large and then it is promptly detected when it appears, as it is presented in the right plot, which shows how the CUSUM remains close to 0 until it start drifting upward at second 40 and it crosses the threshold. The threshold is set to fix a false alarm rate of 1 hour, which with a sampling rate of 10 MHz and snapshot time of 20 ms becomes equal to $h_S = 12$ (see dashed black line in Fig. 7).

V. CONCLUSIONS

This paper deals with a twofold objective: on the one hand, a comprehensive overview of quickest detection has been provided with the aim of introducing this topic to the non-expert reader; on the other hand, we have applied the tools of quickest detection theory to a practical example such as interference and multipath detection in GNSS with the aim of improving integrity in single-antenna GNSS receivers. Two different cases have been presented: when the LLR is completely known and when the LLR is unknown. For the first case, the optimal solution is the CUSUM algorithm, whereas for the second case there is not an optimal solution, but a practical approach that works quite well may be the offset-CUSUM. Applying the CUSUM to interference detection we cope with the cases of completely known and unknown LLR, which leads to the use of the CUSUM algorithm and the offset-CUSUM, respectively. These algorithms are applied to two different metrics, the kurtosis and the chi-squared GoF test, respectively. The first is relevant for PW/CW interferences (i.e. it is restricted to the type of interference), but it uses the optimal algo-

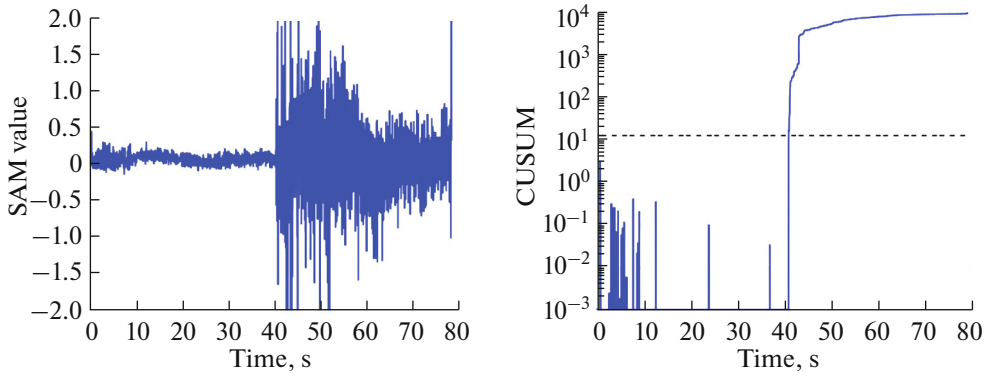

Fig. 7. SAM-based multipath detection for the real data characterized in Fig. 6. Metric (left) and CUSUM (right) time-evolution.

rithm. The GoF method is not restricted to any kind of interference, but it does not use the optimal algorithm, and then it may be used as complement for the cases when the kurtosis is not useful. On the other hand, applying the CUSUM to multipath detection we cope with the case of incompletely known LLR. In this case, we see that we can discriminate between LOS and NLOS conditions. This is done by making use of two different CUSUM for detecting both the change in mean and variance of the SAM. Results of the proposed methods show the suitability of quickest detection for interference and multipath detection and the potential interest in practical applications involving GNSS signal integrity real-time monitoring. This is so because the suggested methods make use of simple techniques (i.e. easy for practical implementation) and allow tuning the CUSUM algorithm providing certain performance in terms of false alarms or detection delay fixed by the user through the detection threshold.

APPENDIX

Proof of Theorem 3

In order to prove the bounds in (31) let J be the stopping time of a one-sided test

$$J = \inf\{j : Z_j > h\}, \tag{56}$$

for some test statistics $\{Z_j\}$, which are function of the i.i.d. observations $x(j)$ (i.e. $Z_j = q(x(j))$). For $k = 1, 2, \ldots$, let J_k be the stopping time of the same test applied to $\{Z_j\}$ for $j \geq k$ and define N as

$$N = \min_{k\geq 1}\{J_k + k - 1\}, \tag{57}$$

the stopping time of the test that stops when the first of the tests applied to $\{Z_j\}$ $\forall j \geq k$ for $k = 1, 2, \ldots$ stops. Now, we quote the following useful lemma, a proof of which is found in [18].

Lemma. *Let J be such that* $\Pr\{J < \infty | H_0\} \leq \alpha$. *Then,*

$$\mathrm{E}\,[N|\mathcal{H}_0] \geq 1/\alpha, \tag{58}$$

and for any alternative distribution,

$$\mathrm{E}\,[N|\mathcal{H}_1] \leq \mathrm{E}\,[J|\mathcal{H}_1]. \tag{59}$$

To use the lemma, we examine the Wald's one-sided test with stopping variable J defined by

$$J = \inf\{m : \tilde{S}_0^m > h\}, \tag{60}$$

where

$$\tilde{S}_0^m = \sum_{i=0}^{m} \rho(x(i)). \tag{61}$$

The probability that this test terminates (i.e., $\Pr\{J < \infty\}$) is the probability that the boundary h is exceeded. For the case of $\rho(n) = \mathrm{LLR}(n)$, this probability can be computed using the theory of sequential detection [23]. However, this probability cannot be computed exactly for arbitrary jumps $\rho(n)$. In this case, we can only provide an estimate using Wald's approximations and bounds [20, 21, 23].

Therefore, in order to compute the probabilities and expectations required in the lemma for J, we consider the two-sided Wald test with boundaries $-\epsilon < 0 < h$ given by the stopping time M,

$$M = \inf\{m : \tilde{S}_0^m < -\epsilon \quad \text{or} \quad \tilde{S}_0^m > h\}, \tag{62}$$

with $\tilde{S}_0^m$ as in (61). The one-sided test in (56) is now the limit of the two-sided test in (62) as ε tends to infinity (i.e. $\lim_{\epsilon\to\infty} M = J$). Let us formally define the OC of the two-sided test according to

$$\mathrm{P}_\theta(M) = \Pr\{\tilde{S}_0^m < -\epsilon\}. \tag{63}$$

The following bound for the OC will be used under $\mathcal{H}_0$ [20, 23]:

$$\mathrm{P}_{\theta_0}(M) \geq \frac{e^{\omega_0 h} - 1}{e^{\omega_0 h} - \eta e^{-\omega_0 \epsilon}}, \tag{64}$$

where $\eta \leq 1$, and $\omega_0 > 0$ is the root of the equation $\mathrm{E}_0[\epsilon^{\omega\rho(n)}] = 1$. Also, we will use the following bound for the ASN under $\mathcal{H}_1$ [20, 23]

$$\mathrm{E}_1(M) \le \frac{-\epsilon \mathrm{P}_{\theta_1}(M) + h[1 - \mathrm{P}_{\theta_1}(M)]}{\mathrm{E}_1[\rho(n)]}. \quad (65)$$

Hence, the probability that J does not stop under $\mathcal{H}_0$ is given by the limit as ϵ tends to infinity of the probability that M terminates at the lower threshold $-\epsilon$:

$$\begin{aligned} &\Pr\{J = \infty \big| \mathcal{H}_0\} \\ &= \lim \mathrm{P}_{\theta_0}(M) \ge \frac{e^{\omega_0 h} - 1}{e^{\omega_0 h}} = 1 - e^{-\omega_0 h}. \end{aligned} \quad (66)$$

Therefore, the probability that J terminates is upper bounded by

$$\Pr\{J < \infty \big| H_0\} \le e^{-\omega_0 h}. \quad (67)$$

Similarly, for the ASN of the one-sided test we have:

$$\begin{aligned} &\mathrm{E}_1[J] \\ &= \lim_{\epsilon \to \infty} \mathrm{E}_1[M] \le \lim_{\epsilon \to \infty} \frac{-\epsilon \mathrm{P}_{\theta_1}(M) + h[1 - \mathrm{P}_{\theta_1}(M)]}{\mathrm{E}_1[\rho(n)]}. \end{aligned} \quad (68)$$

The right hand side is a decreasing function of $\mathrm{P}_{\theta 1}(M)$, so that the inequality is preserved if we replace $\mathrm{P}_{\theta 1}(M)$ by zero, resulting in

$$\mathrm{E}_1[J] \le \frac{h}{\mathrm{E}_1[\rho(n)]}. \quad (69)$$

Now, the lemma can be applied to yield results on the offset-CUSUM with a threshold h and using $\rho(n)$ instead of LLR(n). It is worth mentioning that N is equivalent to the stopping time T^* defined in (18), and then we can show that $\tilde{t}_a = N$, with $Z_j = \tilde{S}_0^j = \sum_{i=1}^{j} \rho(x(i))$, so that the mean time between false alarms and the mean delay for the offset-CUSUM in (29) are bounded by

$$\begin{aligned} \overline{T} &= \mathrm{E}_0[N] \ge e^{\omega_0 h}, \\ \overline{\tau} &= \mathrm{E}_1[N] \le \frac{h}{\mathrm{E}_1[\rho(n)]}. \end{aligned} \quad (70)$$

ACKNOWLEDGMENTS

This work was partly supported by the Spanish Government under grant TEC2014-53656-R and by the European Commission under the IGNSSRX project.

REFERENCES

1. Seco-Granados, G., López-Salcedo, J.A., Jiménez-Baños, D., and López-Risueño, G., Challenges in indoor global navigation satellite systems, *IEEE Signal Processing Magazine,* 2012, vol. 29, no. 2, pp. 108–131.
2. Parkinson, B.W. and Spilker, J.J., *Global Positioning System: Theory and Applications*, vol. 2, AIAA, 1996.
3. Balaei, A.T. and Dempster, A.G., A statistical inference technique for GPS interference detection, *IEEE Transactions on Aerospace and Electronic Systems*, 2009, vol. 45, no. 4, p. 1499.
4. Lee, H.K. et al., GPS multipath detection based on sequence of successive-time double-differences, *IEEE Signal Processing Letters*, 2004, vol. 11, no. 3, pp. 316–319.
5. Broumandan, A., Jafarnia-Jahromi, A., Dehghanian, V., Nielsen, J., and Lachapelle, G., GNSS spoofing detection in handheld receivers based on signal spatial correlation, in *Proc. IEEE Position, Location and Navigation Symposium (PLANS)*, 2012, pp. 479–487.
6. Magill, D., Optimal adaptive estimation of sampled stochastic processes, *IEEE Transactions on Automatic Control*, 1965, vol. 10, no. 4, pp. 434–439.
7. Blom, H., An efficient filter for abruptly changing systems, in *Proc. IEE 23rd Conference on Decision and Control*, 1984, no. 23, pp. 656–658.
8. Koshaev, D., Kalman filter-based multialternative method for fault detection and estimation, *Automation and Remote Control*, 2010, vol. 71, no. 5, pp. 790–802.
9. Broumandan, A., Jafarnia-Jahromi, A., Daneshmand, S., and Lachapelle, G., Overview of spatial processing approaches for GNSS structural interference detection and mitigation, *Proceedings of the IEEE*, 2016, vol. 104, no. 6, pp. 1246–1257.
10. Calmettes, V., Pradeilles, F., and Bousquet, M., Study and comparison of interference mitigation techniques for GPS receiver, in *Proc. 14th International Technical Meeting of the Satellite Division of The Institute of Navigation* (ION GPS 2001), 2001, pp. 957–968.
11. Bhuiyan, M.Z.H., Lohan, E.S., and Renfors, M., Code tracking algorithms for mitigating multipath effects in fading channels for satellite-based positioning, *EURASIP Journal on Advances in Signal Processing*, 2007, vol. 2008, no. 1, pp. 1–17.
12. Braasch, M.S., Performance comparison of multipath mitigating receiver architectures, in *Proc. IEEE Aerospace Conference*, vol. 3, 2001, pp. 1309-1315.
13. Mubarak, O.M. and Dempster, A.G., Exclusion of multipathaffected satellites using early late phase, *Journal of Global Positioning Systems*, 2010, vol. 9, no. 2, pp. 145–155.
14. Mertikas, S.P., Automatic and online detection of small but persistent shifts in GPS station coordinates by statistical process control, *GPS Solutions,* 2001, vol. 5, no. 1, pp. 39–50.
15. Osklper, T. and Poor, H.V., Quickest detection of a random signal in background noise using a sensor array, *EURASIP Journal on Applied Signal Processing,* 2005, no. 1.
16. Lifeng, L., Yijia, F., and Poor, H.V., Quickest detection in cognitive radio: A sequential change detection framework, in *Proc. IEEE Global Communications Conference (GLOBECOM)*, 2008, pp. 1–5.
17. Page, E.S., Continuous inspection schemes, *Biometrika*, 1954, vol. 41, pp. 100–115.
18. Lorden, G., Procedures for reacting to a change in distribution, *The Annals of Mathematical Statistics*, 1971, vol. 42, no. 6, pp. 1897–1908.

19. Moustakides, G.V., The Annals of Statistics, *The Annals of Statistics,* 1986, vol. 14, no. 4, pp. 1379–1387.
20. Basseville, M. and Nikiforov, I.V., *Detection of Abrupt Changes: Theory and Application,* Prentice Hall, 1993.
21. Poor, H.V. and Hadjiliadis, O., *Quickest Detection*, Cambridge, 2009.
22. Egea-Roca, D., Seco-Granados, G., and López-Salcedo, J.A., On the use of quickest detection theory for signal integrity monitoring in single-antenna GNSS receivers, in *Proc. International Conference on Localization and GNSS (ICL-GNSS)*, 2015, pp. 1–6.
23. Wald, A., Sequential tests of statistical hypotheses, *The Annals of Mathematical Statistics,* 1945, vol. 16, no. 2, pp. 117–186.
24. Egea-Roca, D. et al., Signal-level integrity and metrics based on the application of quickest detection theory to interference detection, in *Proc. 28th International Technical Meeting of The Satellite Division of the Institute of Navigation* (ION GNSS+), 2015, pp. 3136 – 3147.
25. Egea-Roca, D. et al., Signal-level integrity and metrics based on the application of quickest detection theory to multipath detection, in *Proc. 28th International Technical Meeting of The Satellite Division of the Institute of Navigation* (ION GNSS+), 2015, pp. 2926–2938.
26. D'Agostino, R.B. and Stephens, M.A., *Goodness-of-Fit Techniques*, CRC Press, 1986.
27. De Roo, R.D., Misra, S., and Ruf, C.S., Sensitivity of the kurtosis statistic as a detector of pulsed sinusoidal radiofrequency interference in a microwave radiometer receiver, in *Proc. IEEE International Geoscience and Remote Sensing Symposium (IGARSS),* 2007, vol. 45, no. 7, pp. 2706–2709.
28. Lopez-Salcedo, J.A., Parro-Jimenez, J. M., and Seco-Granados, G., Multipath detection metrics and attenuation analysis using a GPS snapshot receiver in harsh environments, in *Proc. IEEE European Conference on Antennas and Propagation (EuCAP)*, 2009, pp. 3692–3696.